

Crosslinkable Branched Hydrazones as Potential Hole Transporting Materials

Zbig Tokarski¹, Nusrallah Jubran¹, Vytautas Getautis², Osvaldas Paliulis²,
Maryte Daskeviciene², Ingrida Paulauskaite², Vygintas Jankauskas³,
Valentas Gaidelis³, and Jonas Sidaravicius⁴

¹Samsung Information Systems America, Woodbury, Minnesota

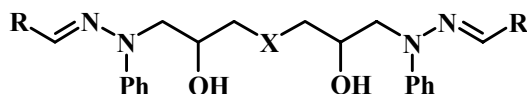
²Kaunas Univ. of Technology, Faculty of Chemical Technology, Kaunas, Lithuania

³Vilnius University, Department of Solid State Electronics, Vilnius, Lithuania

⁴Vilnius Gediminas Technical University, Vilnius, Lithuania

Abstract

A novel family of hole transporting materials (TM) having the following structure was developed and evaluated for electrophotography.



General structure

Such branched hydrazone compounds were synthesized by the reaction of N-2,3-epoxypropyl-N-phenylhydrazones, having heterocyclic or aromatic chromophores R, with different linking agents X, for example, benzenediols or aromatic dimercapto compounds. The molecules of these TM consist of two hydrazone branches linked by the central flexible bridge. The existence of several diastereoisomers, the possibility of intermolecular hydrogen bonding and flexibility of aliphatic linking chains make crystallisation in solid state difficult, so these materials are molecular glasses. Another peculiarity of these TM is the presence of two hydroxyl groups in the molecule. This improves adhesion and compatibility not only with traditional polycarbonate (PC) binder material but also with polyvinylbutyral (PVB). Meanwhile, such branched hydrazone dimers can be chemically crosslinked in the layer, for example, by reaction of the hydroxyl groups with polyisocyanates. These branched hydrazone properties increase the layer stability to bending and stretching of electrophotography belts and the effects of liquid developer. The synthesized TM and compositions with binder exhibit good hole transporting properties and high mobility making them useful for preparation of high sensitivity electro-photographic photoconductors.

Introduction

Low molecular TM compounds are usually crystalline materials, are not capable of forming thin neat homogenous layers, and must be used in combination with polymeric binders. The presence of a large proportion of binder in the compositions, usually 50 % of the total composition mass, leads to considerable decrease of carrier mobility. Even in such compositions, the possibility of the TM crystallisation remains and this causes problems during electrophotographic layer (EPL) preparation and extended printing. Another problem, which arises with preparation of the belt format EPL on flexible supports, is bending and stretching stability of the layers. This problem is especially acute in machines with liquid development, because liquid developer promotes crack formation. Another problem is TM solubility in liquid developer which leads to deterioration of both EPL and liquid developer during printing. Solving of these problems requires TM with special molecule design and improved properties.

For electrophotographic applications during the 1980's, we synthesized well defined low-molar-mass photoconductive compounds that are capable of forming amorphous films on substrates, including flexible ones.¹ Such compounds are prepared by the reaction of oxiranes containing photoconductive groups with different bifunctional compounds such as aromatic diols, dimercapto compounds, and derivatives of aniline.

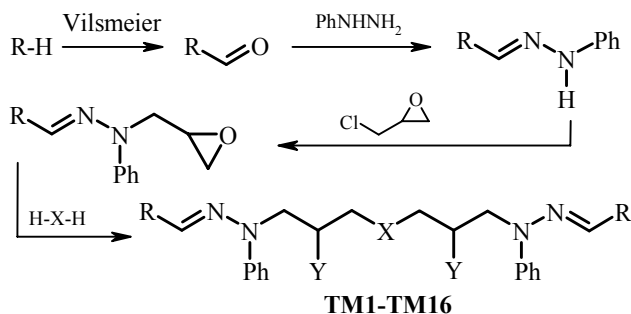
Here we report on the synthesis, characterisation and photoconductive properties of a novel family of hole TM. The molecules of these TM consist of two branches with hydrazone chromophores linked by the central group. The molecular structure of these TM makes crystallization in the solid state difficult, allowing these materials to form molecular glasses. Another peculiarity of these TM is presence of two -OH groups in molecule. This improves adhesion and compatibility with various binders, including PC and PVB. These TM can be used with binder, without

binder in the case of solid substrate, or with low binder concentrations.

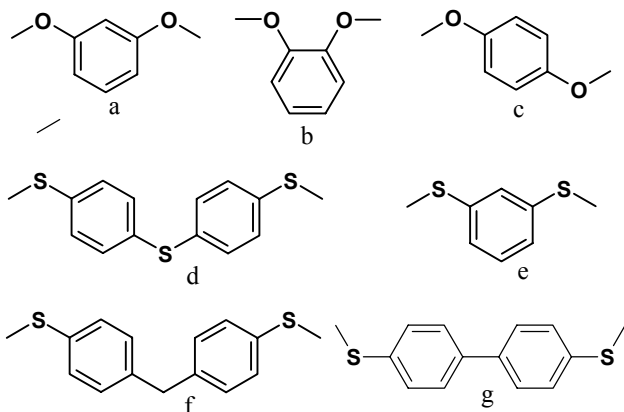
Experimental

Synthesis

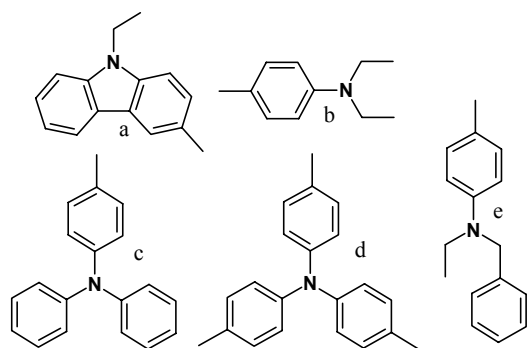
The syntheses of the branched hydrazones **TM1-TM16** were done in the 4-step reaction sequence shown below.



The structures of the central connecting groups X are



and those of the chromophores R are



The first step was the Vilsmeier reaction followed by the reaction with phenylhydrazine. The next step is N-alkylation of hydrazone with epichlorohydrin and the final step is formation of the dimer. An addition step (alkylation of hydroxyl groups with iodoethane) was done in the case of **TM16**. The details of synthesis and spectral data of TM are reported.^{2,3}

Table 1. Composition and parameters of the branched hydrazones TM1-TM16

TM	X	Y	R	T_m (°C)	T_g (°C)	I_p (eV)
1	a	OH	a	145	80	5.35
2	b	OH	a	-	78	
3	c	OH	a	214	89	
4	d	OH	a	147; 185	84	5.39
5	e	OH	a	101	30	5.35
6	f	OH	a	107	81	5.35
7	g	OH	a	242	61	5.36
8	a	OH	b	60	51	5.11
9	b	OH	b	-	46	5.04
10	c	OH	b	67	58	5.11
11	d	OH	b	155	54	5.10
12	a	OH	c	89; 106	82	5.43
13	d	OH	c	134; 187	80	5.34
14	d	OH	d	81; 126	83	5.21
15	d	OH	e	118	51	5.24
16	a	OEt	a	-	64	5.41

Measurement

The phase transitions of **TM1-TM16** were investigated by the differential scanning calorimetry (DSC) method on Perkin Elmer DSC-7, Mettler Star DSC822 or TA Instruments Model 2929 DSC (New castle, DE) apparatus. Samples of 3-12 mg as obtained from synthesis were heated in aluminium pans at a scan rate 10 K/min under a nitrogen flow. During the first heating the melting points were measured. After melting, the samples were cooled with the same rate. The resulting glasses were heated again under the same conditions to measure the glass transitions.

Ionization potential was measured by the photo-emission in air method described in Ref. 4.

The samples for mobility measurements were prepared with most of the TM listed in Table 1, with the exception of **TM3** and **TM7** which were nearly insoluble. The branched hydrazones are able to form stable layers without binder, so samples for mobility measurements were prepared from neat TM and from 1:1 mass proportion compositions of TM with various binders. The various types of polyvinylbutyral and polycarbonate include PVB1 from Aldrich PVB 41,843-9 with average $M_w=70,000 - 100,000$ and 18-20 wt. % of hydroxyl groups; PVB2 from Sekisui S-LEC B BX-1; PVB3 from Sekisui S-LEC B BX-5; PVB4 from Solutia PVB B-79 with average $M_w=50,000 - 70,000$ and 10.5-13 wt. % of hydroxyl groups; and PC-Z from Mitsubishi Gas Chemical Co. polycarbonate Iupilon Z-200. All TM investigated here form transparent layers with all these binder, with the exception of **TM16** with substituted hydroxyl groups. The samples for mobility measurements were prepared by coating TM solutions or solutions of the TM compositions with binder in THF on polyester film with conductive Al layer. The layer thickness was in the range 5-10 μm . The cross-linked samples were prepared from composition of TM, PVB1 and polyisocyanate Desmodur

L75 of Bayer AG (DEL) in wt. proportion 70:15:15. The samples were heated at 120°C for 0.5 h to cross-link.

The hole drift mobility was measured by time of flight technique.^{5,7} Positive corona charging created electric field inside the TM layer. Charge carriers were generated at the layer surface by illumination with pulses of nitrogen laser (pulse duration was 2 ns, wavelength 337 nm). The layer surface potential decrease as a result of pulse illumination was up to 1-5 % of initial potential before illumination. The capacitance probe that was connected to the wide frequency band electrometer measured the speed of the surface potential decrease dU/dt . The transit time t_t was determined by the kink on the curve of the dU/dt transient in linear or double logarithmic scale. The drift mobility was calculated by the formula $\mu = d^2/U_0 t_t$, where d is the layer thickness and U_0 is the surface potential at the moment of illumination.

Results and Discussion

Formation of the glassy state of **TM1-TM16** was confirmed by DSC analysis. The melting points (T_m) and glass transition temperatures (T_g) of synthesized TM are presented in Table 1. These investigations revealed that some of the branched hydrazones can exist both in crystalline and amorphous state while others were found only in amorphous phase in our experiments. The DSC curve for **TM3** at first heating reveals a number of polymorphous changes before melting at 214°C (Fig. 1). No crystallization takes place during cooling or second heating, only glass transition at 89°C is revealed in the second heating. This means that the material remains in glassy state after melting and subsequent cooling. This is common feature for all the branched hydrazones investigated here. The glassy state of these materials is quite stable; no signs of crystallization were detected in the glassy layers during over year storage at ambient conditions. Glass transition occurs at 78°C but no melting is seen for **TM2** (Fig. 2), this means that the original state of the sample was amorphous.

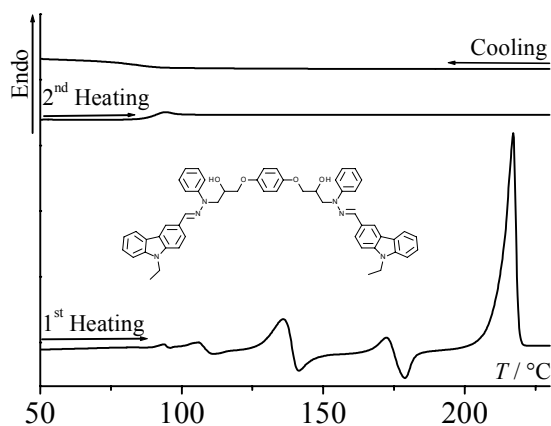


Figure 1. DSC curves of **TM3** (heating and cooling rate 10 K/min).

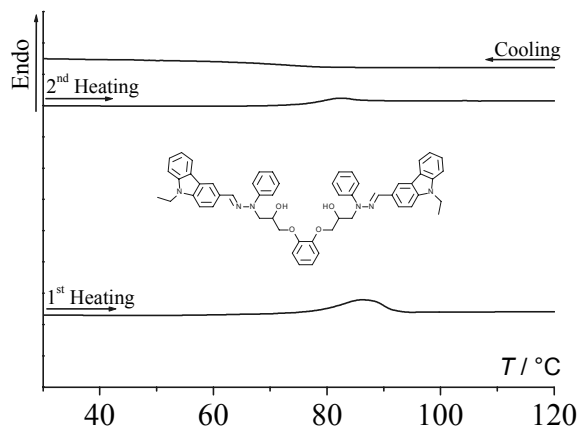


Figure 2. DSC curves of **TM2** (heating and cooling rate 10 K/min).

The comparison of the DSC analysis results for the **TM1-TM3**, reveals a significant role of the substitution of benzene at the central connecting group. In the case of *para* substitution in **TM3**, the melting point is over 200°C and the material is polymorphic. The melting enthalpy is high, the material is practically insoluble in common organic solvents, except highly polar solvents such as dimethyl formamide. A similar situation exists in the case of **TM7** with a biphenyl group at the center. On the other hand **TM2** with *ortho* substituted benzene ring was found only in amorphous state and its glass transition point is lower than that of **TM3**. These facts indicate significance of the molecule symmetry.

Another important factor influencing morphological state of the TM is the presence or absence of hydroxyl groups. **TM1** and **TM16** differ between themselves only in this aspect. The **TM16** with substituted hydroxyl groups was found only in amorphous state, while **TM1**, in which these groups are present, exists in crystalline state. The glass transition point of the **TM16** (64°C) is considerably lower as compared with **TM1** (80°C, Table 1). All this is, obviously, caused by hydrogen bond formation between the -OH groups in **TM1** and absence of them in **TM16**.

The structure of the charge transporting chromophores also has significant influence on melting and glass transition points of the TM. As seen from Table 1, these temperatures are lower for the TM with chromophores **b** and **e** as compared with others. TM with chromophores **c** and **d** usually have two melting points. This means that there are different crystalline forms of these TM and transitions of one into another take place during first heating.

The photoemission in air spectra for some of the branched hydrazones are shown on Fig. 3, ionization potential values are presented in Table 1. There is little ionization potential (I_p) difference depending on the central connecting group, the charge transporting groups are determining its value. The lowest I_p values, about 5.1 eV, were observed in the TM with chromophore with diethyl aniline group (**b**). Replacement of this group by ethylbenzyl aniline group leads to increase of I_p by more

than 0.1 eV. Ionization potential of the TM with carbazole or triphenylamine groups is 5.3-5.4 eV.

Table 2. Mobility data

Layer composition	μ_0 (cm^2/Vs)	μ (cm^2/Vs)	α (cm/V) ^{0.5}
TM1	$4 \cdot 10^{-8}$	$5.8 \cdot 10^{-6}$	0.0062
TM1+PVB1, 1:1	$1.0 \cdot 10^{-9}$	$3 \cdot 10^{-7}$	0.0072
TM4	$1.3 \cdot 10^{-7}$	$1.3 \cdot 10^{-5}$	0.0058
TM4+PVB1, 1:1	$2.8 \cdot 10^{-9}$	$5.2 \cdot 10^{-7}$	0.0065
TM4+PVB1+DEL, 70:15:15	$1.6 \cdot 10^{-9}$	$6.0 \cdot 10^{-7}$	0.0074
TM5	$2.3 \cdot 10^{-7}$	$1.1 \cdot 10^{-5}$	0.0048
TM5+PVB1, 1:1	$4.0 \cdot 10^{-9}$	$2.4 \cdot 10^{-7}$	0.0050
TM6	$6.0 \cdot 10^{-8}$	$8.8 \cdot 10^{-6}$	0.0063
TM6+PVB1, 1:1	$6.3 \cdot 10^{-9}$	$3.8 \cdot 10^{-7}$	0.0051
TM8	$7.0 \cdot 10^{-8}$	$1.5 \cdot 10^{-5}$	0.0068
TM8+PVB1, 1:1	$2.0 \cdot 10^{-9}$	$2.7 \cdot 10^{-7}$	0.0061
TM9	$8.0 \cdot 10^{-8}$	$1.4 \cdot 10^{-5}$	0.0065
TM10	$1.3 \cdot 10^{-7}$	$3.3 \cdot 10^{-5}$	0.0068
TM11	$2.2 \cdot 10^{-7}$	$2.3 \cdot 10^{-5}$	0.0058
TM11+PVB1+DEL, 70:15:15	$5.0 \cdot 10^{-9}$	$1.0 \cdot 10^{-6}$	0.0065
TM12	$2.4 \cdot 10^{-6}$	$1.3 \cdot 10^{-4}$	0.0050
TM13	$5 \cdot 10^{-6}$	$2.6 \cdot 10^{-4}$	0.0050
TM13+PVB1, 1:1	$6.2 \cdot 10^{-8}$	$2.0 \cdot 10^{-6}$	0.0044
TM13+PVB2, 1:1	$5.5 \cdot 10^{-8}$	$2.0 \cdot 10^{-6}$	0.0045
TM13+PVB3, 1:1	$5.8 \cdot 10^{-8}$	$1.8 \cdot 10^{-6}$	0.0043
TM13+PVB4, 1:1	$6.3 \cdot 10^{-8}$	$2.5 \cdot 10^{-6}$	0.0046
TM13+PC-Z, 1:1	$1.7 \cdot 10^{-7}$	$4.9 \cdot 10^{-6}$	0.0042
TM13+PVB1+DEL, 70:15:15	$1.0 \cdot 10^{-7}$	$1.9 \cdot 10^{-6}$	0.0037
TM14	$9.0 \cdot 10^{-6}$	$4.7 \cdot 10^{-4}$	0.0049
TM14+PVB1+DEL, 70:15:15	$1.8 \cdot 10^{-7}$	$4.0 \cdot 10^{-6}$	0.0038
TM15	$3.8 \cdot 10^{-7}$	$1.7 \cdot 10^{-5}$	0.0048
TM15+PVB1, 1:1	$1.3 \cdot 10^{-8}$	$5.8 \cdot 10^{-7}$	0.0048
TM16	$1.8 \cdot 10^{-7}$	$1.0 \cdot 10^{-4}$	0.0079

Examples of mobility field dependencies are given in Fig. 4. In all the cases investigated, the mobility μ is approximated by the formula

$$\mu = \mu_0 e^{\alpha \sqrt{E}} \quad (1)$$

where μ_0 is the zero field mobility, α is Pool-Frenkel parameter, and E is electric field strength. The mobility defining parameters μ_0 and α values as well as the mobility value at the $6.4 \cdot 10^5$ V/cm field strength are given in Table 2.

While the presence of binder in the TM layer considerably reduces mobility, it has little effect on the mobility field dependence. This is seen on Fig. 4 and in Table 2, where the field dependence defining parameter α is given. In some cases, as with **TM1**, **TM4** and some other TMs, the parameter α is somewhat larger, but in other cases, as with **TM6**, **TM8** and **TM13**, it is even smaller in TM compositions with binder as compared with neat TM.

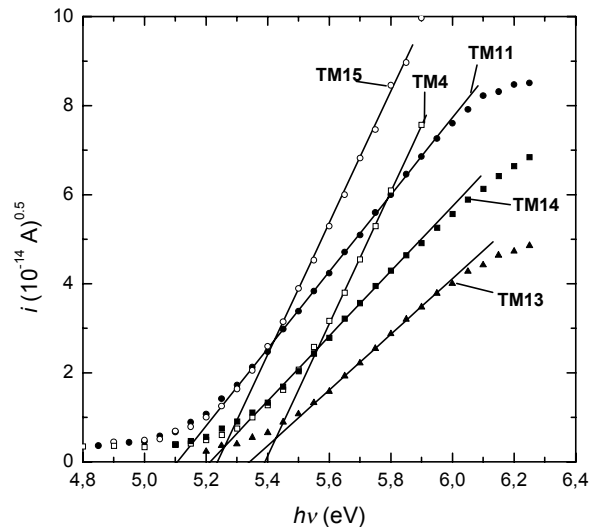


Figure 3. Photoemission in air spectra of branched hydrazones.

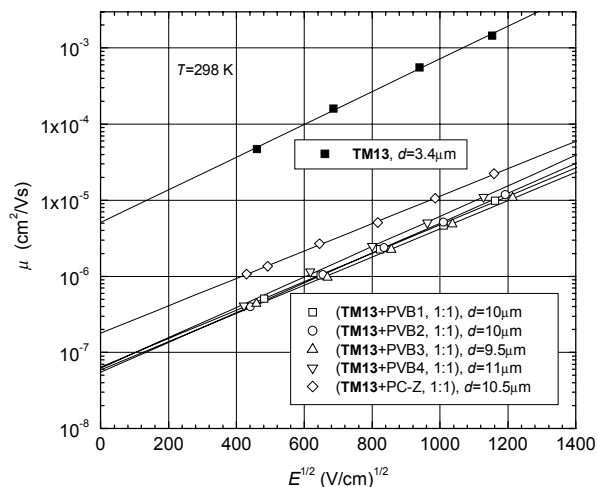


Figure 4. Mobility field dependencies for pure **TM13** and its 1:1 compositions with various binder.

As seen from the results, the mobility value is influenced by a number of factors. First of all mobility is dependent on the charge transporting chromophore nature. The highest mobility values are with chromophores based on triphenylamine (**c**) and dimethyltriphenylamine (**d**) moieties. This is natural because conjugated π electron systems are largest in these chromophores. The other important factor is presence or absence of hydroxyl groups in the TM molecule. This is seen from comparison of mobility for **TM1** and **TM16**. The mobility value for **TM16** is more than by one order of magnitude higher than in **TM1** with these highly polar groups. The effect of polar additives on mobility in molecularly doped polymers is known, but not well explained.⁸ Probably, the observed difference between the materials with and without the hydroxyl groups is of a similar nature. The presence of hydroxyl groups may

be not desirable in the sense of carrier mobility but other positive aspects of the TM with such groups, as improved adhesion, compatibility with various binder, and stability to liquid developer may be more important. It is necessary to note that the mobility in a number of TM investigated as well as compositions with binder is high enough for many practical applications. The mobility of these TM can be increased by using a lower binder concentration.

The central connecting group (X) also affects hole mobility; however, this influence is much weaker in comparison with chromophores. The highest mobility for the TM group with carbazole containing chromophores is with sulphur compounds in the centre of molecule. The same occurs for the TM group with diethylaniline containing chromophores, albeit the difference in this group is smaller. The **TM14** with dimethyltriphenylamine containing chromophores and the centre **d** has the highest mobility among TM investigated.

Mobility in the compositions of TM with binder is considerably lower as compared with neat TM. The difference can be up to two orders of magnitude. Figure 4 and Table 2 show the **TM13** composition with polycarbonate binder has the highest mobility. Mobility in this case is about 2-2.5 times higher as compared with various PVB binders. The hydroxyl groups present in PVB, probably, contributed to this decrease. The advantageous properties offered by the presence of hydroxyl groups in PVB are good adhesion, improved crazing stability to bending and stretching, and deterring the effects of liquid developer may outweigh loss of mobility.

The xerographic time of flight transients for the cross-linked samples were of disperse character but the transit time was well seen on lg-1g plots. The hole mobility measurement results for cross-linked compositions are presented on Fig. 5 and in Table 2. The mobility values for a strong electric field, as a rule, are close to the values in the compositions with PVB. However, the concentration of TM in the uncross-linked compositions is 50 wt.% as compared to 70 wt. % in cross-linked compositions. This means that cross-linking is affecting the mobility more than the simple addition of binder. Mobility field dependence for **TM11** and **TM4** is somewhat stronger and it is weaker in the cross-linked compositions for **TM13** and **TM14**.

According to widely used charge transport models in molecularly doped polymers mobility and its field dependence are determined by the energetic and positional disorders in the transporting composition. The mobility data in the molecular solids are usually interpreted in terms of the Borsenberger, Pautmeier and Bäessler formula:⁹

$$\mu(E, T) = \mu_0' \exp\left[-\left(\frac{2\sigma}{3kT}\right)^2\right] \exp\left\{C\left[\left(\frac{2\sigma}{3kT}\right)^2 - \Sigma^2\right] E^{1/2}\right\}. \quad (2)$$

Here, μ is the mobility, σ is the energy width of the hopping site manifold, which provides a measure of the energetic disorder, Σ is the degree of positional disorder, E the electric field, μ_0' is a mobility pre-factor. It is evident from this formula that the zero field mobility $\mu(0, T)$ is

determined by the energetic disorder σ , while mobility field dependence is caused by the difference between the energetic disorder σ and positional disorder Σ dependent terms in the formula.

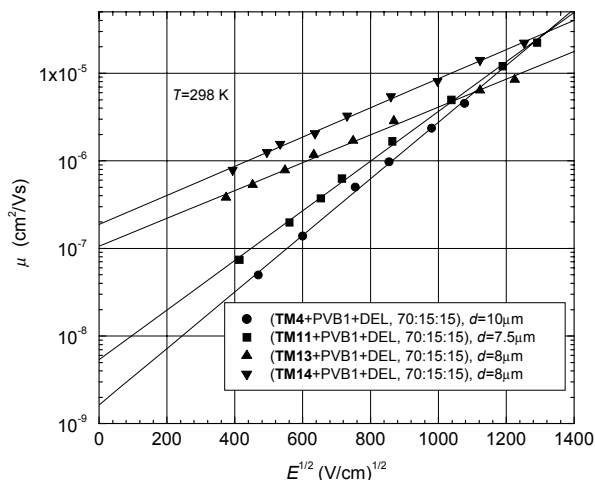


Figure 5. Hole mobility field dependencies in cross-linked compositions.

The mobility of both neat TM and in compositions with binder materials was investigated. To interpret our experimental data, we assumed that the introduction of the binder lead to an increase of both of energetic and positional disorders but that the difference

$$\Delta = (2\sigma / 3kT)^2 - \Sigma^2 = \alpha / C \quad (3)$$

in formula (2) changed slightly despite a considerable change of both terms.

Dunlap, Kenkre and Paris¹⁰ proposed another charge carrier transport model in organic transporting media giving a Poole-Frenkel type of field dependence described by formula (1). There is no positional disorder in this model and energetic disorder is considered as correlated disorder originally defined by Novikov and Vannikov.¹¹ Energetic disorder is evident by the presence of smooth troughs and valleys caused by the action of dipole moments. The expression for mobility is¹⁰

$$\mu = \mu_0 \exp\left[-(\sigma / kT)^2 + \gamma E^{1/2}\right], \quad (4)$$

$$\gamma = [4\sigma^2 ea / (kT)^3]^{1/2}. \quad (5)$$

where a is scaling factor of the magnitude close to intermolecular distances. This model gives new opportunities to interpret mobility data in organic transporting compositions. Usually there is a large concentration of polar groups in transporting compositions. Charge transporting chromophores have their own dipole moments. For example compounds **2** and **9** in¹² are close analogues of chromophores **TM4** and **TM13** of this

investigation. The dipole moments of these compounds are 2.57 and 2.35D respectively¹². In addition, there are polar hydroxyl groups in the central connecting bridges of the TM. Polar groups are present in the polycarbonate and polyvinylbutyral binders, so the concentration of polar groups in the TM and transporting compositions is high and this should be an important factor in determining the properties of the organic transporting materials.

Conclusions

A series of new glass-forming hydrazones containing diethylaniline, benzylethylaniline, ethylcarbazole, triphenylamine and dimethyltriphenylamine moieties have been synthesized by the reaction of different bifunctional compounds with N-2,3-epoxypropyl derivatives of phenylhydrazones of corresponding aromatic aldehydes. The molecular structure of these branched hydrazones prevents TM crystallization, allows for the preparation of stable films without binder material or with a low binder concentration, and is compatible with polycarbonate and polyvinylbutyral binders. The hydroxyl groups also allow for cross-linking of these transporting materials in the layer. The hole mobility of both neat TM and compositions with binder materials have been studied. The highest hole mobility, reaching 10^{-4} cm²/Vs at $6 \cdot 10^5$ V/cm electric field, was observed in the TM with dimethyltriphenylamine or triphenylamine moieties.

References

1. M. Daskeviciene, V. Getautis, J.V. Grazulevicius, A. Stanisauskaite, J. Antulis, V. Gaidelis, V. Jankauskas, J. Sidaravicius, *J. Imaging Sci. and Technol.*, **46**, 467 (2002).
2. V. Getautis, M. Daskeviciene, A. Stanisauskaite, O. Paliulis, *Chemistry of Heterocyclic Compounds*, **7**, 884 (2002).
3. V. Getautis, O. Paliulis, I. Paulauskaite, V. Gaidelis, V. Jankauskas, J. Sidaravicius, Z. Tokarski, K. Law, N. Jubran, *J. Imaging Sci. and Technol.*, (in preparation).
4. S. Grigalevicius, G. Blazys, J. Ostrauskaite, J.V. Grazulevicius, V. Gaidelis, V. Jankauskas, E. Montrimas, *Synthetic Metals*, **128**, 127 (2002).
5. E. Montrimas, V. Gaidelis, A. Pazera. *Lithuanian Journal of Physics*, **6**, 569 (1966).

6. Vaezi-Nejad, S. M., *Int. J. Electronics*, **62** No 3 361-384 (1987).
7. Archie Y. C. Chan and C. Juhasz, *Int. J. Electronics*, **62**, No 4, 625-632 (1987).
8. R. H. Yang, J. J. Fitzgerald, *J. Chem. Phys.*, **102** (15), 6290 (1995).
9. P. M. Borsenberger, L. Pautmeier, H. Bässler, *J. Chem. Phys.*, **94**, 5447-5454 (1991).
10. D. H Dunlap, V. M Kenkre, P. E. Paris, *J. Imag. Sci. Technol.*, **43**, No 5, 432 (1999).
11. S. V Novikov, A. V. Vannikov, *Synth. Met.*, **85**, 1167 (1997)
12. A. Fuji, T. Shoda, S. Aramaki, T. Murayama, *J. Imag. Sci. Technol.*, **43**, No. 5, 430, (1999).

Biographies

Dr. Vytautas Getautis studied chemical technology at Kaunas University of Technology, Lithuania. In 1985 he entered post-graduate studies of Organic chemistry and in 1988 defended his doctoral thesis, entitled "Synthesis of 1,3-Diheterocyclyl- or Aryl-, Heterocyclyl-2-propanol Glycidyl Ethers and 1,3-Dioxolanes". Since 1989 he works as a senior research associate and since 1995 as an Associate Professor at the Department of Organic chemistry of Kaunas University of Technology. His research interests include the synthesis and properties of photoconductive molecular glasses and investigation of the products of the interaction of aromatic amines and heterocyclic compounds with epichlorohydrin. He published 5 patents and 17 scientific papers.

Zbig Tokarski received his Ph.D. in Chemical Engineering from the University of Connecticut, Storrs, CT in 1990. He has worked on optical organic material research at Wright Patterson Air Force Base for 9 years and on electrophotographic materials and physics for the last 7 years, first with Imation Corp and now with Samsung Electronics. Dr. Tokarski is currently a senior group leader with Samsung Information Systems America, Digital Printing Solutions Laboratory, Woodbury, Minnesota. His main research activities involve all areas of electrophotography.

Correspondence on this paper should be e-mailed to ztokarski@mn.sisa.samsung.com